Karaelmas Fen ve Mühendislik Dergisi
Journal home page: http://fbd.beun.edu.tr

Research Article

The Study of REMD Simulation of SEB-Binding Repetitive Peptide Sequences

SEB'e Bağlanan Tekrarlı Peptid Dizilimlerinin REMD Çalışması

Nesrin Kılıç*, Kadir Demir

Department of Physics, Bülent Ecevit University, Zonguldak, Turkey

Abstract

We investigated whether the conformational differences of modified peptides play a role for affinity or not. For this purpose, we have performed the replica exchange molecular dynamic simulation (REMD) to obtain the conformational states and secondary structural propensities of repetitive peptide sequences changed the affinity of binding to staphylococcal enterotoxin B (SEB). The results obtained from REMD simulations have shown that the secondary structures of these repetitive peptide sequences were mainly random coil, bend and turn structures with a small amount of helix and β-bridge structures for all temperatures. Besides it was shown that, with repeating the sequence, while the percentage of random coil structures decreased, the ones of bend structures increased. These results are consistent with the ones which obtained from circular dicroism spectroscopy. In terms of principal component analysis (PCA), the free energy landscapes of peptide sequences were obtained and found several local minima. The secondary structures corresponding with these minima have mainly coil, turn and bend structures for both peptides. In addition to these dominant structures considerable amount of helix and β-bridge structures were also outstanding. Its observed that while the number of repetition of peptide sequence increases, the percentage of random coil structures are decreases and this transformation in the random coil structures emerges in the form of increases in the rates of bend, turn, helix and β-bridge structures with the chosen temperature and region. The results pointed that it was not monitored a directly relationship between the affinity and secondary structures propensities of repetitive peptides.

Keywords: Free energy landscape, Peptide ligands, Principal component analysis, Replica exchange molecular dynamics, SEB-binding peptides, Secondary structure

Öz

Değişikliğe uğramış peptitlerin konformasyonel farklılıklarının, afinite üzerinde rol oynayıp oynamadığını araştırdık. Bu amaçla, staphylococcal enterotoxin B (SEB)'e bağlanma afinitesini değiştiren tekrarlı peptit dizilimlerinin ikincil yapı eğilimlerini ve konformasyonel durumlarını elde etmek için Replica Exchange Moleküler Dinamik (REMD) simülasyonlar yaptık. REMD simülasyonlardan elde edilen sonuçlar bu tekrarlı peptit dizilimlerinin ikincil yapılarının tüm sıcaklıklar için az miktarda heliks ve β-bridge yapılarla birlikte çoğunlukla random coil, bend ve turn yapılar olduğunu gösterdi. Bunların yanısıra, dizilimlerin tekrarlanmasıyla random coil yapıların yüzdesi azalırken, bend yapılarda artış gözlenmiştir. Bu sonuçlar Circular Dicroism (CD) spektroskopiden elde edilen sonuçlarla uyumludur. Temel Bileşen Analizi (PCA) vasıtasıyla, peptit dizilimlerinin serbest enerji yüzeyleri elde edilmiş ve birkaç yerel minimum bulunmuştur. Bu minimumlara karşılık gelen ikincil yapılar her iki peptit için de çoğunlukla coil, bend ve turn yapılara sahiptir. Bu baskın yapılara ek olarak bir de önemli miktarda heliks ve β-bridge yapılar göze çarpmıştır. Peptit dizilimlerini tekrar sayısı arttıkça random coil yapıların yüzdesi azalır ve random coil yapılardaki bu dönüşüm seçilen sıcaklık ve bölgeye bağlı olarak bend, turn, heliks ve β-bridge yapılardaki artış şeklinde ortaya çıkar. Sonuçlar, tekrarlı peptit dizilimlerinin ikincil yapı eğilimleri ve afinite arasında doğrudan bir ilişki görüntülenemediğini işaret etmiştir.

Anahtar Kelimeler: Serbest enerji yüzeyi, Peptit ligand, Temel bileşen analizi, Kopya değiş-tokuş moleküler dinamik, SEB'e bağlanan peptitler, İkincil yapı

*Corresponding author: nesrinkilicf@hotmail.com

Received / Geliş tarihi : 11.08.2016
Accepted / Kabul tarihi : 13.01.2017

1. Introduction

Staphylococcal enterotoxin B (SEB), produced by Staphylococcus aureus, is a toxin causing food poisoning in humans. This toxin is potential biological warfare agent due to its high thermal stability (Marrack and Kappler 1990). Hence, it is need to the rapid, sensitive and cost-effective detection method. On the other hand, SEB has been detected by enzyme-linked immunosorbent assay (ELISA) (Hahn et.al. 1986, Park et.al.1994) and immunosensors based on piezoelectric crystal sensors (Harteveld et.al. 1997, Lin and Tsai 2003), surface plasmon resonance (SPR) sensors (Homola et.al. 2002, Naimushin et.al. 2002, Slavik et.al. 2002) and fiber optic sensors (King et.al. 1999). However, these methods used antibodies with high costs and time consuming for detection of SEB. Therefore, peptide ligands were investigated as novel recognition agents.

Phage-displayed peptide libraries have been used for determination of peptide ligands with a high affinity to SEB by Dudak et.al. (2010). The selected 12-mer peptides were investigated by circular dichroism (CD) spectroscopy and conventional Molecular Dynamics (MD) (Dudak et.al. 2010). However, when compared to affinities of antibodies, their affinities are still lower. In later study, we have used modified forms of the peptides used previously to increase the affinities to SEB (Dudak et.al. 2012). The modifications were done by repeating the 12-mer peptide sequences. The affinities of modified peptides to SEB were obtained by isothermal titration calorimetry (ITC). Also, we investigated the binding of a modified peptide by SPR sensor to confirm the affinity increase. In addition, the secondary structures of peptides were analyzed MD simulation and CD spectroscopy. As results of the study, it was reported that the conformation of peptides might be associated with affinities of peptides.

However, with conventional MD simulations at low temperatures, a protein or peptide generally becomes trapped in any of many local energy minima. Replica Exchange Molecular Dynamics (REMD) is a commonly used computational method for efficient sampling of the phase of large biomolecular systems. Replica exchange algorithm was introduced to protein simulations by Hansmann (1997). Sugita and Okamato first extended the algorithm to Molecular Dynamics simulations (Sugita and Okamoto 1999).

In REMD, each replica at different temperatures is simulated simultaneously and independently in parallel. At regular time intervals, an exchange of current conformations of a pair of neighboring replicas is attempted and is accepted or rejected according to generalized Metropolis rule. Therefore, it is possible to escape from local energy traps by allowing random walks (Swendsen and Wang 1986, Geyer 1992, Hukushima and Nemoto 1996).

In this study, we have studied REMD simulations of two modified peptides called Peptide3M2 and Peptide3M3. Peptide3M2 and Peptide3M3 are duplicate and triplicate of Peptide3 respectively, which has high affinity to SEB, with sequence Leu^{1}-Leu^{2}-Ala^{3}-Asp^{4}-Thr^{5}-Thr^{6}-His^{7}-His^{8}-Arg^{9}-Pro^{10}-Trp^{11}-Thr^{12}. The results of later study showed that while affinity of duplicate of peptide approximately 10-fold increased, affinity of triplicate of peptide decreased (Dudak et.al. 2012). To investigate how the modification primary structure of peptide effect affinity to SEB, the secondary structures obtained REMD simulations were analyzed at different temperatures. Because the hydrophobic effect is the dominant force in protein folding (Pace et.al. 1996), we have calculated the solvent accessible areas (SASAs). In addition, due to hydrogen bonding plays an important role on stabilizing proteins we also analyzed the average number of hydrogen bond as a function of temperature.

Free energy landscapes (FELs) are vital for our understanding of biological and chemical processes such as solvation phenomena (Mobley et.al. 2009), protein-ligand association (Limongelli 2012, Mobley and Klimovich 2012), enzymatic reactions (Warshel 1981) and membrane-water partitioning (Swift and Amaro 2013). REMD simulations based on atomic -level contain a great number of degrees of freedom. One way to overcome this problem is to use the reaction coordinates for the description of biological systems. One of the most commonly used method for obtaining reaction coordinates is the principal component analysis (PCA) which typically captures most of the total displacement by means of the first few principal components (PCs) (Maisuradze et.al. 2009, Maisuradze and Leitner 2007). By PCA, the conformational probability distributions and FELs were determined.

2. Method

The TINKER molecular modelling package (Ren and Ponder 2002) was used to construct our peptides named Peptide3M2 and Peptide3M3. All simulations are performed using the GROMACS molecular modeling package (Van der Spoel et.al. 2005) in conjunction with OPLS-AA force field (Jorgensen and Severance 1990).

The MD simulations were initially started from extended (primary) geometries without any bias where the peptides were terminated with N-terminal NH_3^+ and the C-terminal COO^- group. In order to remove close van der Waals contacts we have firstly minimized the energy of both peptides system *in vacuo*. This minimization consisted from the steepest descent to conjugate gradient mode. To improve conformational sampling in molecular dynamics simulations, we have secondly heated the systems to high temperature and then have cooled to room temperature in constrained simulating annealing *in vacuo*. After this step, the last frames were chosen as the starting structure for each peptide. Then these structures were solvated with single point charge water model (SPC) (Berendsen et.al. 1981) in a cubic box an edge length of 3 nm. The solvated systems contain 2868 and 3653 water molecules for Peptide3M2 and Peptide3M3, respectively. The solvated configuration energy was again minimized from the steepest descent to conjugate gradient methods. Then in order to reach stability we have performed a short MD simulation and finally the obtained configurations were submitted to REMD production simulation for each peptide. The REMD simulations having 2 fs time step were performed for Peptide3M2 and Peptide3M3 with 64 different replicas in the temperature range of 280-511 K and 280-501 K, respectively (as 256 ns total simulation time for each peptide). Replica exchange was tried every 500 MD steps with exchange probability 0.2 and 0.15 during the REMD simulations for Peptide3M2 and Peptide3M3, respectively. The other protocols which followed during these simulations are given a detailed manner in our previous work (Demir et.al. 2014).

The used temperatures for all the replicas are

280.00, 282.92, 285.86, 288.82, 291.81, 294.82, 297.86, 300.92, 304.00, 307.12, 310.25, 313.41, 316.59, 319.80, 323.04, 326.30, 329.59, 332.90, 336.24, 339.61, 343.01, 346.43, 349.88, 353.36, 356.87, 360.41, 363.97, 367.56, 371.18, 374.84, 378.52, 382.22, 385.96, 389.73, 393.54, 397.37, 401.24, 405.13, 409.06, 413.02, 417.01, 421.03, 425.08, 429.17, 433.29, 437.45, 441.64, 445.86, 450.12, 454.41, 458.73, 463.09, 467.48, 471.92, 476.39, 480.90, 485.44, 490.02, 494.64, 499.28, 503.98, 508.71, 513.48, 518.29 for Peptide3M2 and

280.00, 282.87, 285.77, 288.69, 291.63, 294.58, 297.57, 300.57, 303.60, 306.65, 309.73, 312.83, 315.95, 319.10, 322.27, 325.46, 328.68, 331.92, 335.18, 338.47, 341.79, 345.13, 348.51, 351.90, 355.32, 358.77, 362.24, 365.74, 369.26, 372.81, 376.39, 380.00, 383.64, 387.30, 390.99, 394.72, 398.47, 402.25, 406.05, 409.89, 413.75, 417.65, 421.57, 425.53, 429.51, 433.53, 437.58, 441.66, 445.77, 449.91, 454.08, 458.29, 462.53, 466.80, 471.11, 475.45, 479.82, 484.23, 488.67, 493.15, 497.65, 502.19, 506.77, 511.40 K for Peptide3M3 (these temperatures were produced from the methods described in Ref. (Patriksson and van der Spoel 2008).

3. Results and Discussion

For Peptide3M3, the potential energy population of each target temperature and the temperature index evolutions of seven representative replicas obtained from our REMD simulations are depicted in Figure 1.

Detecting the sufficient overlap between the energy population and the random walk in the temperature spaces mean that our REMD simulations were performed properly

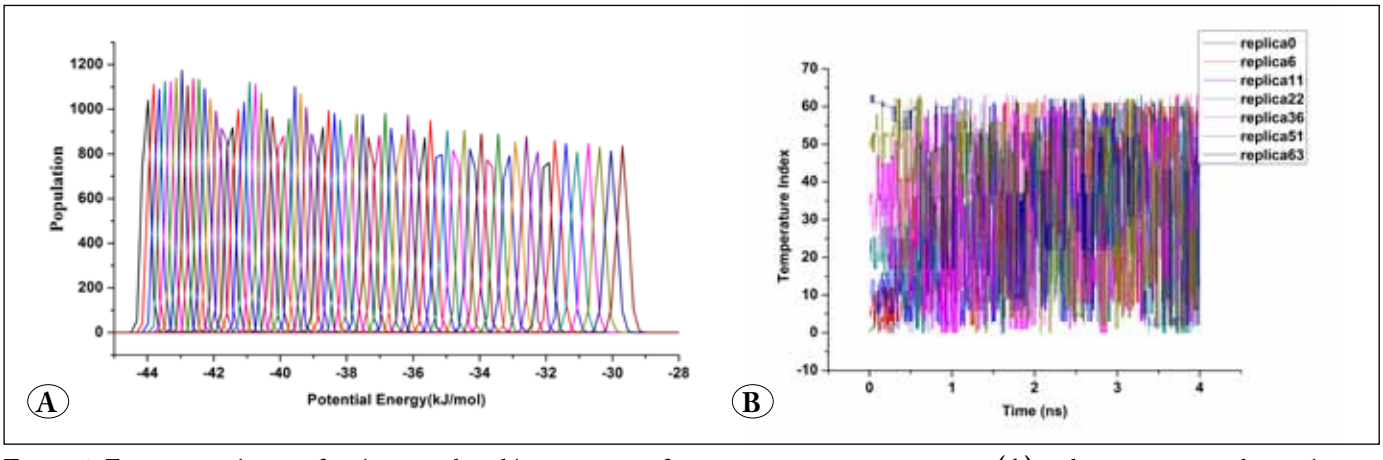

Figure 1. Energy population of replicas produced by sorting configurations to target temperature **(A)** and temperature index evolutions for seven replicas **(B)** for Peptide3M3.

(Hansmann 2010, Kouza and Hansmann 2011). For other peptide sequence similar behaviors have been observed.

3.1. Secondary Structure Analysis

Detecting the types of secondary structures of peptide sequence plays an important role in determining structural and biological properties of peptide. The secondary structures of the peptides in water were characterized by the secondary structure analysis using the definition of proteins protocol (The Dictionary of Secondary Structure of Proteins, DSSP) (Kabsch and Sander 1983). To get insight into secondary structural element types of our peptide sequences and their temperature dependency, we have depicted the secondary structural elements during the simulations for both peptides at four different temperatures.

The secondary structures of Peptide3M2 are given in Figure 2 (a)-(d) at 280, 300, 319 and 518 K temperatures, respectively. The y-axis in the figure corresponds to the residue number.

As seen in Figure 2(a)-(d), Peptide3M2 has shown mostly random coil, bend and turn structures and the first and last residues have random coil structures during the whole simulation time. This situation can be expected due to fact that these terminal residues are in zwitterionic form. As seen Figure 2(a)-(c), while Ala^{3} and His^{20} residues have mostly β-bridge structure, this structure disappears at 518 K. For each of the four temperatures, His^{9}-Thr^{12}, Thr^{16} and Arg^{21}(+) residues generally shown random coil structure. At 280, 300 and 319 K, while the segment Thr^{17}-His^{19} shown bend structure at the first half of simulation, these segments recover the turn and coil at the last half of simulation. In addition to this, a little of helix structure can take place partly in several residues. Peptide3M2 was the duplicate of Peptide3 revealed by repeating the 12-amino acid sequence of the peptide. When compared the first 12 amino acid sequence of Peptide3 and the second one, while the main structures are the same, their locations have differed.

The secondary structures of Peptide3M3 are also given in Figure 3(a)-(d) at 280, 300, 319 and 511 K temperatures, respectively. From Figure 3(a)-(d), it can be seen that the segment Ala^{3}-His^{8} and the segment Thr^{29}-His^{31} adopt mostly the bend structure for each temperatures. Also, the random coil structures appeared in the residues Arg^{9}(+), Leu^{13}, Asp^{16}(-), Thr^{18}-His^{20}, Pro^{22}-Trp^{23} and His^{32} as well the first and last residues. While the β-bridge structures was observed in the residues Leu^{25} and Asp^{28}(-), the turn structures was observed in the residues Leu^{26} and Ala^{27} especially for 280, 300 and 319 K temperatures. In addition, at all temperatures, the residues Arg^{33}(+) and Pro^{34} have a mixture of turn and bend structures. Peptide3M3 was the triplet of Peptide3 revealed by repeating the 12-amino acid sequence of the peptide. It is seen as very rare amino acids protecting their secondary structures in the triplet of peptide as well in the duplicate of peptide.

Analyzing the secondary structures of Peptide3M2 and Peptide3M3 presented in Figure 2 and 3, it is seen that the secondary structures of each amino acid in the first chain of peptide have not remained the same as in the second and the third chains. With repeating the sequence, folding of the peptides in different ways can be expected due to different bonds to be established between amino acid in peptide. As a result, it can be said that this conformational differences may be to play a key role for the binding affinity of peptide.

The percentages of the secondary structures of both peptides are summarized in Table 1 for the four different temperatures. As seen from Table 1, at all temperatures both peptides have mostly random coil, bend and turn structures. In addition to this, a little amount of helix and beta bridge structures was observed for both peptides. Although at all temperatures the percentages of secondary structures didn't change significantly, they have reached their extreme values at 319 K. It was shown that, with repeating the sequence, while the percentage of random coil structures decreased the ones of bend structures increased.

3.2. Hydrogen Bonds and Hydrophobic Forces

We have calculated the average number of intra molecular hydrogen bonds as a function of temperature in order to explore the effect of hydrogen bonding into the conformational structures of both peptides. These are given in Figure 4. As seen from Figure 4(a), the average number of hydrogen bonds for Peptide3M2 reached their maximum value at 339 K and after this temperature it has began to decrease. Similar behavior is also observed for Peptide3M3 (Figure 4(b)).

The hydrophobic force has the dominant effect in protein folding (Dill 1990, Nemethy and Scherage 1962, Pace et.al. 1996). Hence, to assess the hydrophobic forces into the conformational structures of peptide sequences, we have also calculated the contributions of hydrophobic and hydrophilic solvent accessible surface areas (SASA) and their total SASA for both peptides at 300 K.

As seen in Figure 5(a), while the highest hydrophobic contribution was observed at $Trp^{11,23}$, the lowest hydrophobic

contribution was observed at Asp[4, 16](-) for Peptide3M2. The hydrophobic SASAs at the segments Thr[5]-Arg[9](+) and, the same segments in the second sequence of Peptide3M2, the segments Thr[17]-Arg[21](+) remained approximately constant. While the residues His[8] and His[20] provide the highest hydrophilic SASAs, the residues Pro[10], Leu[2] and Ala[3] provide the lowest hydrophilic SASAs (Figure 5(b)). When examined Figure 5(a) and 5(c) together, it is seen that they showed similar behavior. Therefore, it is said that, the total hydrophobic SASAs are greater than the total

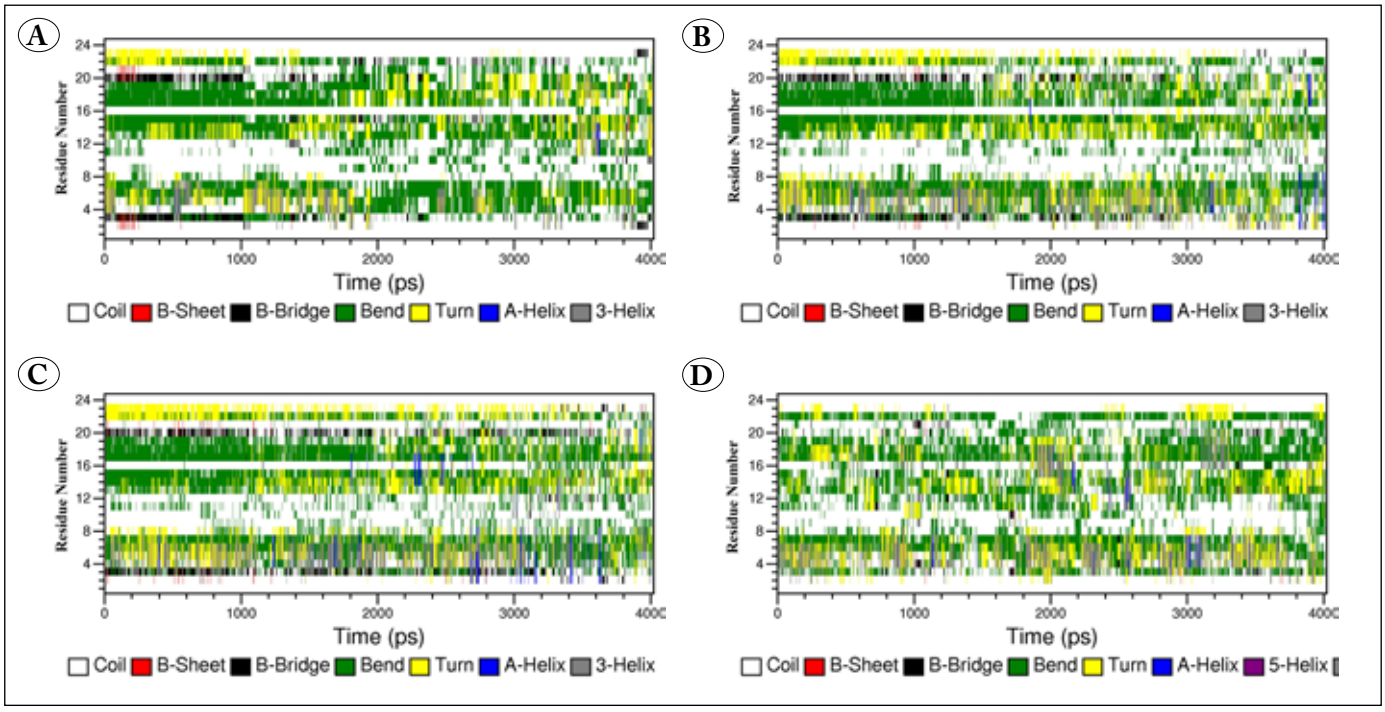

Figure 2. Secondary structures of Peptide3M2 **(A)** 280 K, **(B)** 300 K, **(C)** 319 K and **(D)** 518 K.

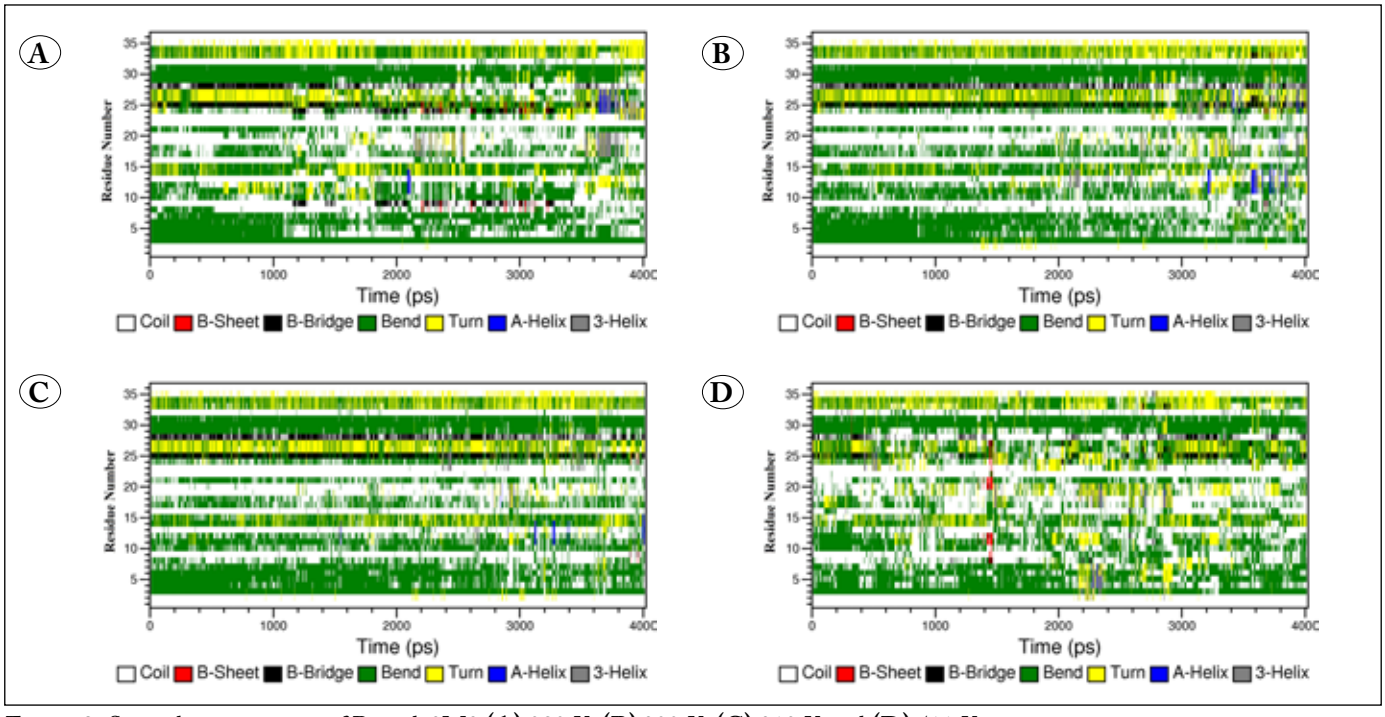

Figure 3. Secondary structures of Peptide3M3 **(A)** 280 K, **(B)** 300 K, **(C)** 319 K and **(D)** 511 K.

Table 1. The averaged population of the secondary structures content from DSSP analysis.

Peptide	T(K)	Coil (%)	Bend (%)	Turn (%)	Helix (%)	β- Sheet (%)	β-Bridge (%)
*Peptide3	280	59.4	23.5	11.0	3.6	0.0	2.48
	300	58.7	24.1	10.7	4.3	0.0	2.17
	501	61.1	28.2	8.35	1.6	0.2	0.56
Peptid3M2	280	53.1	31.0	9.8	2.93	0.25	2.82
	300	52.3	28.2	12.0	4.54	0.12	2.69
	319	50.7	28.1	12.6	5.10	0.19	3.27
	518	51.8	29.2	12.1	5.68	0.00	1.01
Peptid3M3	280	46.5	38.5	10.1	1.29	0.24	3.21
	300	45.1	39.7	10.4	1.28	0.02	3.38
	319	44.4	41.7	9.7	0.66	0.00	3.43
	511	47.4	39.2	10.5	0.84	0.23	1.28

*Data were taken from our previous study (Demir et.al. 2014).

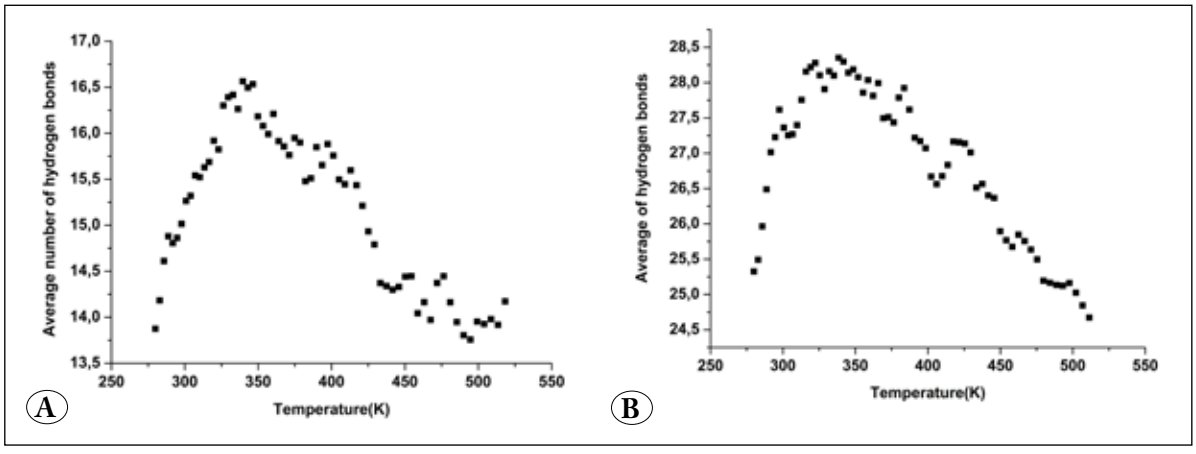

Figure 4. The average number of intra molecular hydrogen bonds for **(A)** Peptide3M2 and **(B)** Peptide 3M3.

hydrophilic SASAs. We have also calculated the number of intermolecular hydrogen bonds per residue of Peptide3M2 at 300 K (Figure 5(d)). While the residues Thr^{24}, Arg^{9}(+), His^{8} and Asp^{4}(-) have high number of hydrogen bond, the residues Pro^{10}, Ala^{3} and Leu^{2} have low number of hydrogen bond.

For Peptide3M3, as in Peptide IIM2, while the highest hydrophobic contribution was observed at $Trp^{35,11}$, the lowest hydrophobic contribution was observed at $Asp^{28,4}$ (-) (Figure 6(a)). As seen in Figure 6(b), while the residues His^{20}, His^{7} and His^{32} provide the highest hydrophilic SASA, the residues Pro^{10}, Leu^{25} and again Pro^{22} give the lowest hydrophilic SASA. For this peptide, the total hydrophobic SASAs are dominant than total hydrophilic SASAs (Figure 6(c)). Figure 6(d) also shows the number of intermolecular hydrogen bonds per residue of Peptide3M3 at 300 K. As seen in the Figure, the residues Thr^{17} and Arg^{21}(+) have the highest number of hydrogen bond. On the other hand, the residues Pro^{10}, Leu^{25} and Pro^{34} have the lowest number of hydrogen bond.

3.3. Principal Components Analysis

By employing the PCA, the eigenvectors of covariance matrix have been calculated. The detailed information about PCA and the calculation of eigenvectors have been presented in our previous work (Demir et.al. 2014).

For PCs calculation, we firstly combined the trajectories of 64 replicas and the average structure was obtained. The resulting average structure was used as reference structure to calculate the eigenvectors corresponding to the princi-

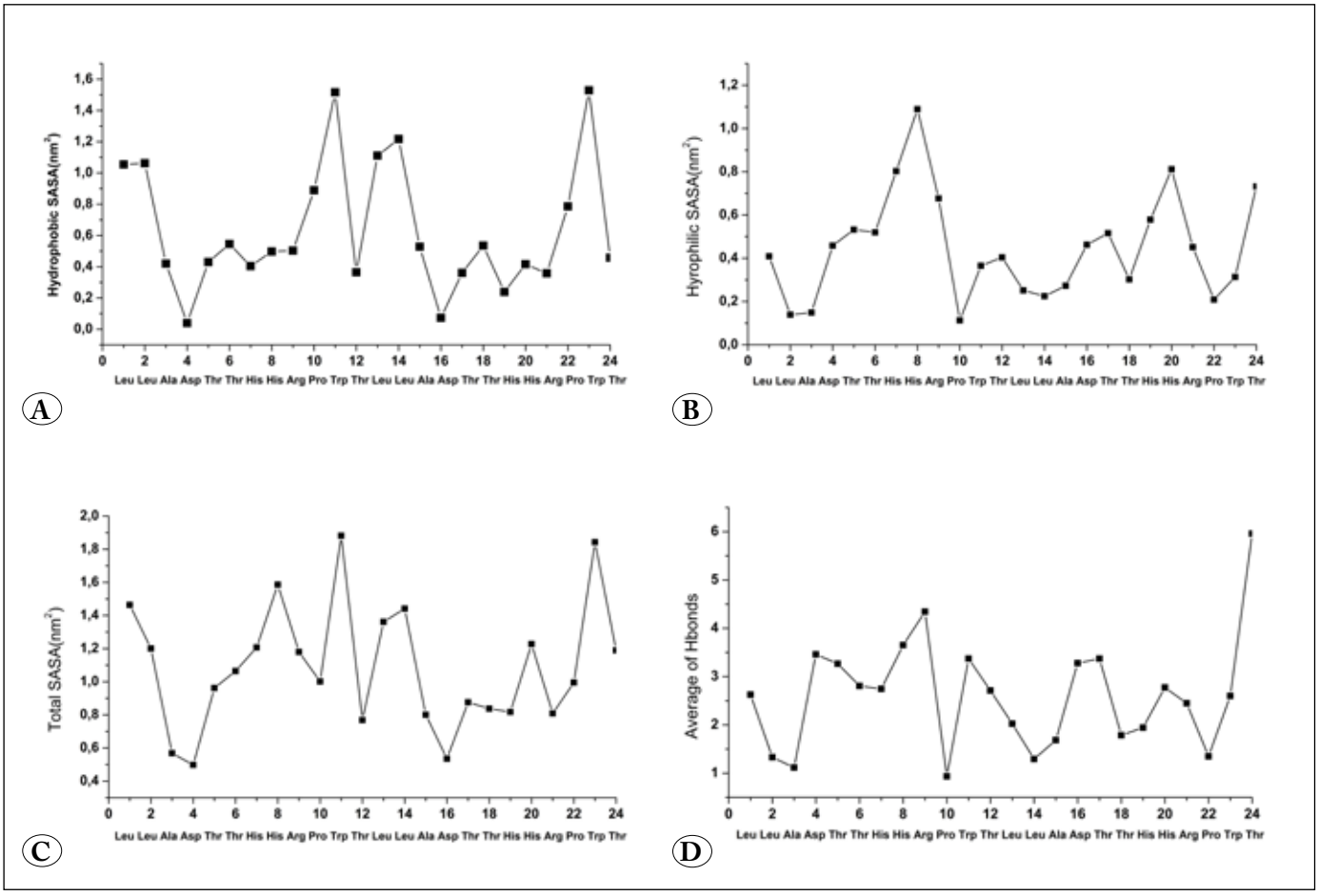

Figure 5. Hydrophobic SASA **(A)**, hydrophilic SASA **(B)**, total SASA **(C)** and average of inter molecular hydrogen bonds **(D)**, for Peptide3M2.

pal components. The calculation of eigenvalues and their projection along the principal components were carried out with respect to the C-alpha atom coordinates of each peptide. The conformational probability distributions obtained from these analyses are given in Figure 7.

According to Figure 7(a), the conformational probability distributions of all replicas for Peptide3M2 with respect the first and second PCs have populated in a certain region which centered near (-1.5; 0.0) and (-1.5; 1.0). One of the representative structures corresponding to the highest probability distributions is shown on the left of the figure. Although for the total motion according to two components the random coil, bend and turn structures are the most dominant secondary structures a small amount of β-bridge and helix structure are seen.

On the other hand according to the first two principal components for Peptide3M3 all trajectories showed the population in the two distinct regions (Figure 7(b)). While the first region having maximum probability is centered around (0.0; 1.5) and (-1.0; 1.0) the second one is centered around (-1.0; 0.0) and (-1.0; 1.0) according to PC1 and PC2, respectively. The representative structures corresponding to these regions are shown on the left and right sides of the figure. While the corresponding structure of the first region has mostly random coil, bend and turn secondary structures the second one, in addition to these three, has also β-bridge structure.

3.4. Free-Energy Landscape

To obtain the conformational dynamics of our modified peptides, free-energy landscapes were obtained in terms of PCA (Figure 8). Free-energy was found as a function of temperature from the equation given as , where P (PC1,T) is the probability distribution obtained from a histogram of simulation data, and k_B is the Boltzmann constant.

To detailed analyses of these free-energy landscapes, for four temperatures, two-dimensional presentation of them as

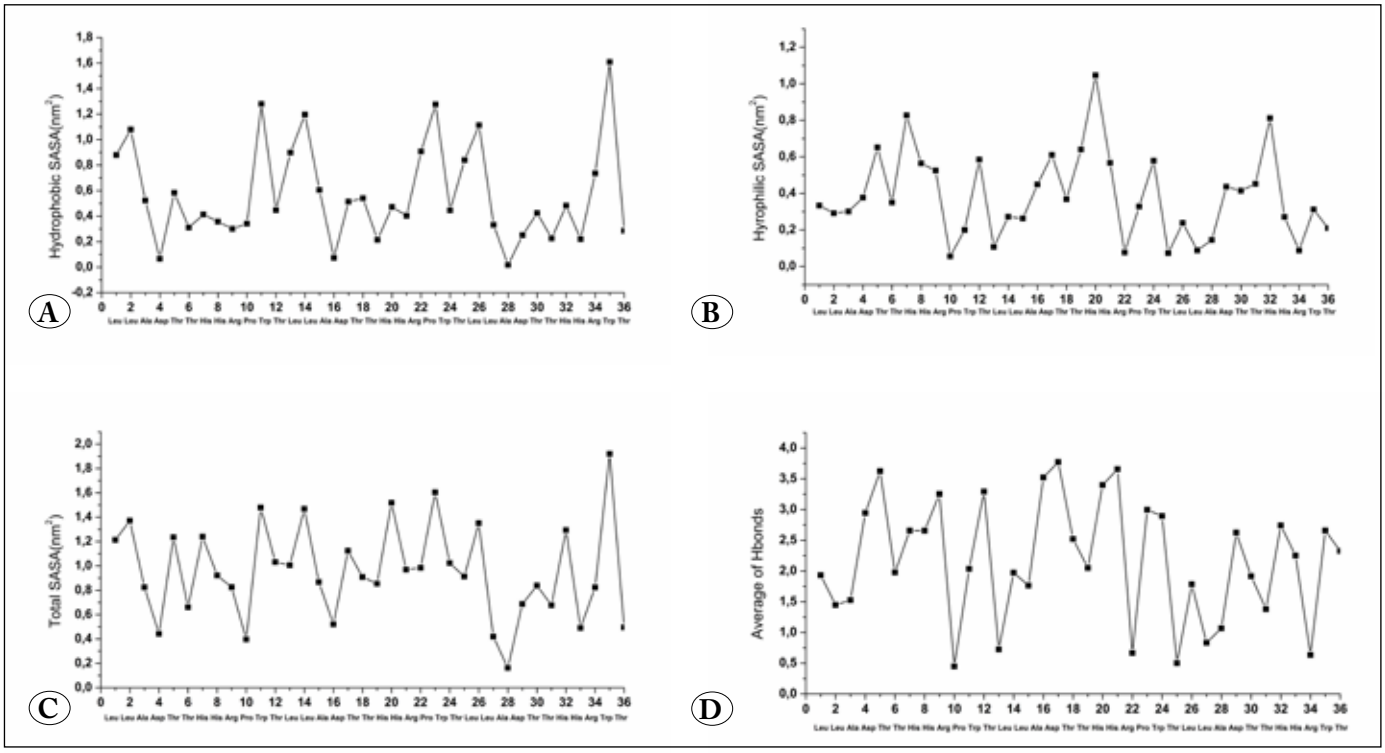

Figure 6. Hydrophobic SASA **(A)**, hydrophilic SASA **(B)**, total SASA **(C)** and average of number of inter molecular hydrogen bonds **(D)**, for Peptide3M3.

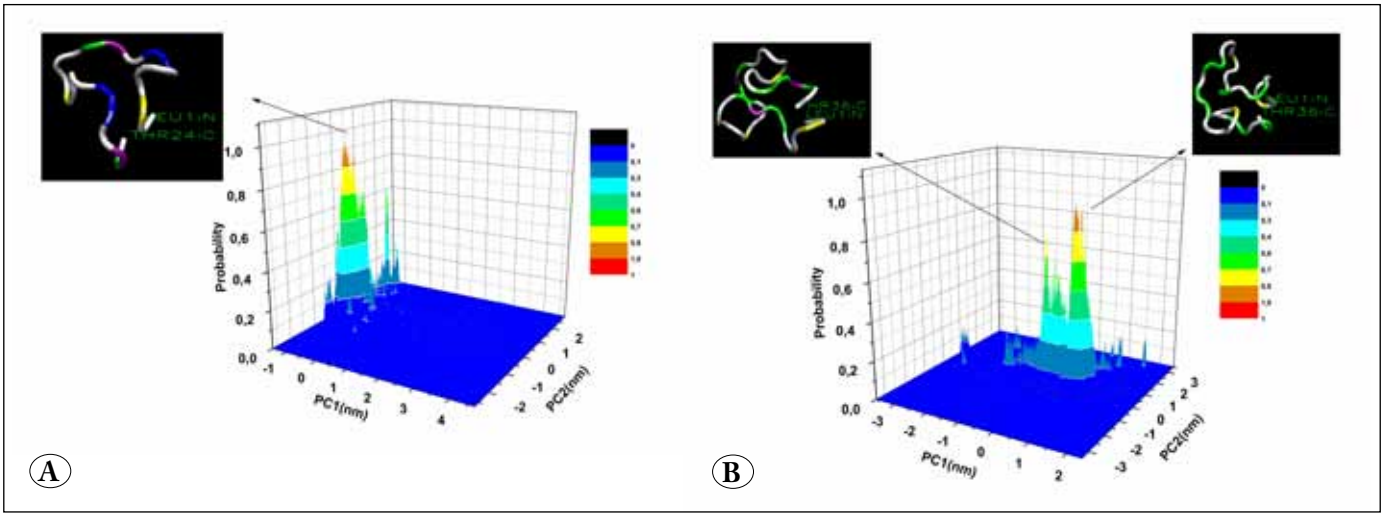

Figure 7. The conformational probability distributions respect to PC1 and PC2 for Peptide3M2 **(A)** and Peptide3M3 **(B)** (The representative structures are visualized by VMD (Humphrey, W.,et.al., 1996), and the residues involved in the turn, random coil, alpha helix, bend, β-bridge are shown by yellow, gray, blue, green and purple respectively).

a function of PC1 were given in Figure 9 for both peptides sequences. It has been shown that there were several obvious minima on the graphs. The calculated percentages of the secondary structures corresponding with these minima were given in Table 2. The ranges of these minima were chosen according to 280 K for both peptides.

As seen in Figure 9(a)-(b) the lowest minima are close to about PC1≈ -1.0 nm and ≈ 1.2 nm for Peptide3M2 and Peptide3M3, respectively. In this figures we have identified four distinct minima that settled at around -1.15 <PC1< -0.60, -0.14 <PC1< 1.00, 1.33 <PC1< 1.60 and 2.08 <PC1< 2.60 for Peptide3M2 and -2.55 <PC1< -1.55, -1.33

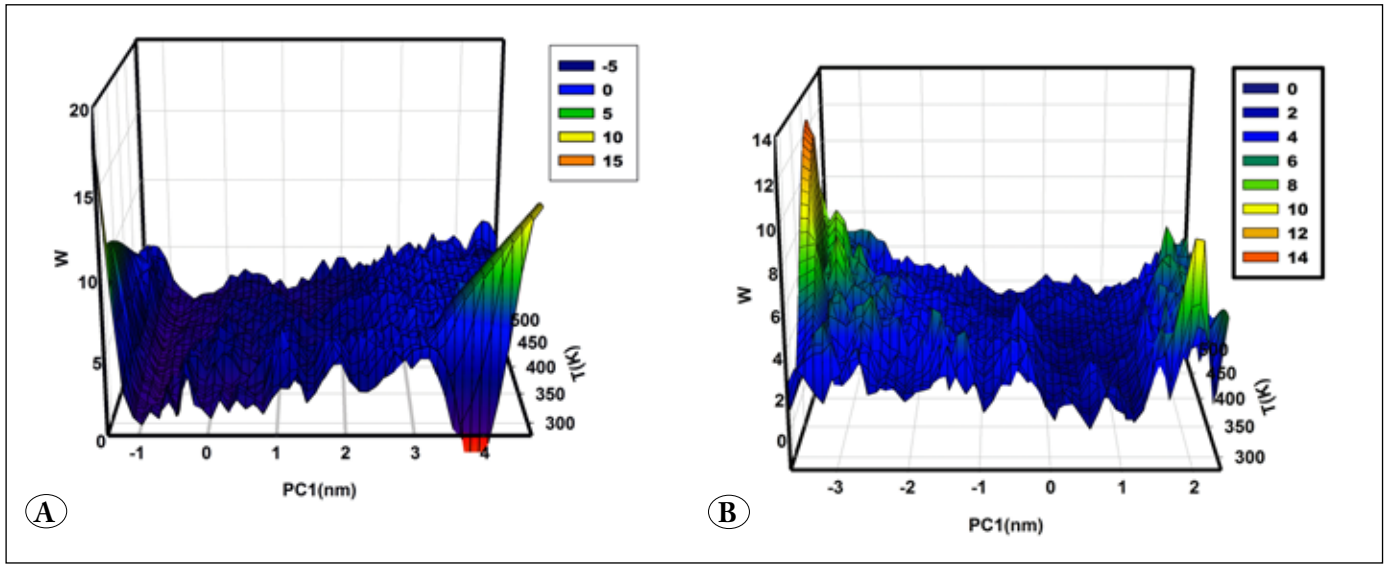

Figure 8. Free-energy landscapes with respect to the first principal component and temperature of **(A)** Peptide3M2 **(B)** Peptide3M3.

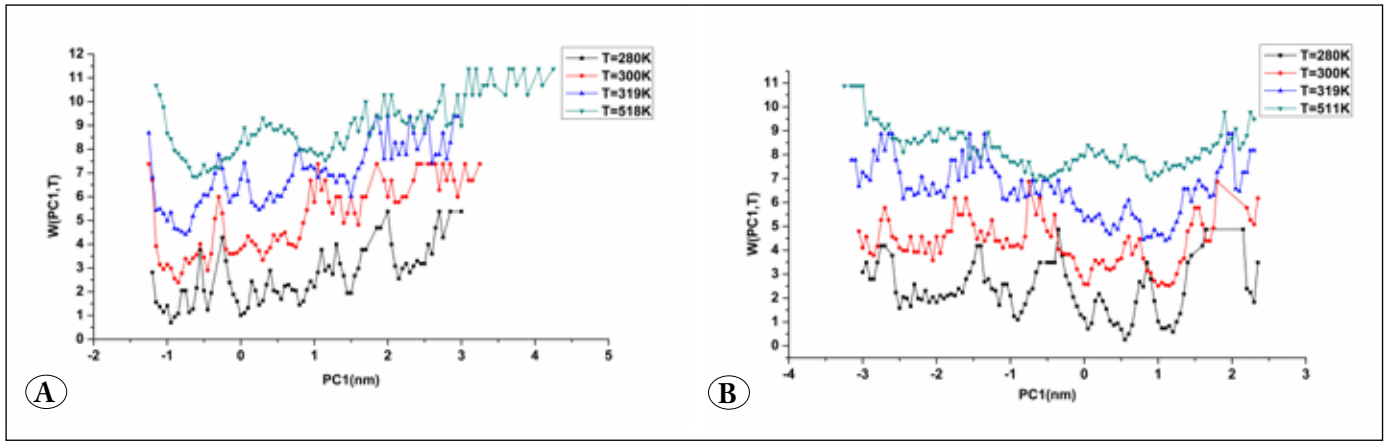

Figure 9. Two-dimensional Free-energy landscapes with respect to the first principal component of Peptide3M2 **(A)** and Peptide3M3 **(B)**, for several temperatures.

<PC1< -0.65, -0.25 <PC1< -0.79 and 0.89 <PC1< 1.39 for Peptide3M3. For each region, mostly dominant secondary structures are random coil, bend and turn structures and the average populations of them change a small amount with the chosen temperature and region (Table 2). In addition to these dominant structures considerable amount of helix and β-bridge structures are also outstanding. İts observed that while the number of repetition of Peptide3 sequence increases, the percentage of random coil structures are decreases and this transformation in the random coil structures emerges in the form of increases in the rates of bend, turn, helix and β-bridge structures with the chosen temperature and region.

4. Conclusions

In our previous study, it has been shown that the repetitive peptide sequences, are duplicate and triplicate of Peptide3, changed the affinity of binding to staphylococcal enterotoxin B (SEB) by experimental methods. In addition to experimental studies, conventional MD simulations were performed for examine structural propensities of peptide sequences. The results of this study showed that while affinity of duplicate of peptide approximately 10-fold increased, affinity of triplicate of peptide decreased (Dudak et.al. 2012).

In this study, to more efficient sampling of the phase space of large bimolecular systems, we have performed the replica

Table 2. The average population of the structures corresponding to local minimum for both peptides (The percentages of structure have been weighted from over the number of configurations of each region).

Peptide	PC1 region (nm)	T (K)	Coil (%)	Bend (%)	Turn (%)	Helix (%)	β–Sheet (%)	β–Bridge (%)
*Peptide3	1.min (0.0; 1.5)	280	57.5	19.1	16.6	6.8	0.0	0.0
		300	57.0	19.9	15.4	8.0	0.0	0.0
	2.min (-0.3; 0.0)	280	62.6	32.0	4.8	0.5	0.0	0.0
		300	60.0	30.0	8.0	1.1	0.0	0.0
	3.min (-1.5;-1.25)	280	57.0	24.9	8.3	0.0	0.0	9.6
		300	54.9	25.9	8.5	0.0	0.5	10.2
Peptide3M2	1.min (-1.15 ; -0.60)	280	50.1	30.3	10.8	2.6	0.0	5.6
		300	49.5	28.3	12.6	4.5	0.0	4.8
	2.min (-0.14 ; 1.00)	280	56.6	32.7	7.4	2.5	0.0	0.8
		300	56.0	29.0	10.9	3.7	0.0	0.4
	3.min (1.33 ; 1.60)	280	57.2	30.9	10.4	0.3	0.0	1.3
		300	55.4	27.3	9.9	4.6	0.0	2.8
	4.min (2.08 ; 2.60)	280	43.4	28.2	17.5	7.8	0.0	2.5
		300	42.4	30.6	17.5	4.3	0.0	5.2
Peptide3M3	1.min (-2.55 ; -1.55)	280	47.8	30.9	15.7	2.6	0.0	3.0
		300	46.5	30.5	13.9	4.2	0.0	4.8
	2.min (-1.33 ; -0.65)	280	42.1	37.6	12.0	4.1	0.0	4.2
		300	44.2	35.6	14.3	1.9	0.0	3.6
	3.min (-0.25 ; -0.79)	280	45.3	41.8	7.8	0.4	0.0	4.2
		300	44.4	41.0	9.9	0.5	0.0	4.3
	4.min (0.89 ; 1.39)	280	49.4	39.8	9.0	0.0	0.0	1.7
		300	45.0	42.9	9.3	0.1	0.0	2.7

exchange dynamic simulation (REMD) for obtained the conformational states of these repetitive peptide sequences. To investigate how the modification primary structure of peptide effect affinity to SEB, the secondary structures obtained REMD simulations were analyzed at different temperatures. At room temperature, the average populations of secondary structures of modified peptides were mainly random coil, bend and turn structures with a small amount of helix and β-bridge structures. It is seen that the secondary structures of each amino acid in the first chain of peptide have not remained the same as in the second and the third chains. With repeating the sequence, folding of the peptides in different ways can be expected due to different bonds to be established between amino acid in peptide.

We have calculated the average number of intra molecular hydrogen bonds as a function of temperature in order to explore the effect of hydrogen bonding into the conformational structures of both peptides. For both peptides, the average number of hydrogen bonds reached their maximum value at 339K temperature and decreased after temperature.

To assess the hydrophobic forces into the conformational structures of peptide sequences, we have also calculated the contributions of hydrophobic and hydrophilic solvent accessible surface areas (SASA) and their total SASA for both peptides at 300 K. It is said that, the total hydrophobic SASAs are greater than the total hydrophilic SASAs for both peptides.

In order to determine structures corresponding to local minima especially at low temperatures, by using PCA, the free energy landscapes of peptide sequences were obtained and found several local minima. The secondary structures corresponding with these minima have mainly coil, turn

and bend structures for both peptides as well considerable amount of helix and β-bridge structures. It is observed that while the number of repetition of peptide sequence increases, the percentage of random coil structures are decreases and this transformation in the random coil structures emerges in the form of increases in the rates of bend, turn, helix and β-bridge structures with the chosen temperature and region.

When our results compared with the experimental results for the affinity, it can be said that a directly relationship between the affinity and secondary structures propensities of duplicate and triplicate repetitive peptides could not be established. To find a correlation between the conformational differences of repetitive peptides and their affinity of binding to SEB, the protein-ligand interactions and binding regions for SEB must be investigated by simulation methods in detail.

5. Acknowledgements

This work was supported by The Scientific Research Fund of Hacettepe University and The Scientific Research Found of Bülent Ecevit University with project numbers 901.602.003 and 2009-13-03-03, respectively.

6. References

Berendsen, HJC., Postma, JPM., van Gusteren, WF., Hermans, J. 1981. Interaction models for water in relation to protein hydration. D. Rediel: Dordrect, 331-342.

Demir, K., Kılıç N., Dudak, FC., Boyacı, İH., Yaşar, F. 2014. The investigation of the secondary structure propensities and free-energy landscapes of peptide ligands by replica exchange molecular dynamics simulations. *Mol. Simul.,* 40: 1015-1025.

Dill, KA. 1990. Dominant forces in protein folding. *Biochemistry*, 29(31):7133-7155.

Dudak, FC., Soykut, EA., Oğuz, ME., Yaşar, F., Boyacı, İH. 2010. Thermodynamic and structural analysis of interactions between peptide ligands and SEB. *J. Mol. Recognit.*, 23: 369–378.

Dudak, FC., Kılıç, N., Demir, K., Yaşar, F., Boyacı, İH. 2012. Enhancing the Affinity of SEB-Binding Peptides By Repeating their Sequence. *Biopolymers (Pept. Sci.),* 98: 145-154.

Geyer, CJ. 1992. Practical Markov chain Monte Carlo. *Stat. Sci*., 7: 473-483.

Hahn, IF., Pickenhahn, P., Lenz, W., Brandis, HJ. 1986. An avidin-biotin ELISA for the detection of staphylococcal enterotoxins A and B. *Immunol Methods*, 92: 25–29.

Hansmann, UHE. 1997. Paralel tempering algorithm for conformational studies of biological molecules. *Chem. Phys. Lett.*, 314: 140-150.

Hansmann, UHE. 2010. Temperature random walk sampling of protein configurations. *Physica A*, 389: 1400-1404.

Harteveld, JLN., Nieuwenhuizen, MS, Wils, ERJ. 1997. Detection of Staphyloccoccal enterotoxin B employing a piezoelectric crystal immunosensor. *J. Microbiol Method*, 7: 661–667.

Homola, J., Dostalek, J., Chen, S., Rasooly, A., Jiang, S., Yee, SS. 2002. Spectral surface plasmon resonance biosensor for detection of staphylococcal enterotoxin B in milk. *Int. J. Food. Microbiol*., 7: 61–69.

Hukushima, K., Nemoto, K. 1996. Exchange Monte Carlo method and application to spin glass simulation. *J. Phys. Soc*., 65: 1604-1608.

Humphrey, W., Dalke, A., Schulten, K. 1996. VMD: Visual molecular dynamics. *J. Mol. Graph.*, 14: 33-38.

Jorgensen, WL., Severance, DL. 1990. Aromatic-aromatic interactions: free energy profiles for the benzene dimer in water, chloroform, and liquid benzene. *J. Am. Chem. Soc.*, 112: 4768-4774.

Kabsch, W., Sander, C. 1983. Dictionary of protein secondary structure: pattern recognition of hydrogen bonded and geometrical features. *Biopolymers*, 22: 2577–2637.

King, KD., Anderson, GP., Bullock, KE., Regina, MJ., Saaski, EW., Ligler, FS. 1999. Detecting staphylococcal enterotoxin B using an automated fiber biosensor. *Biosens. Bioelectron*, 14: 163–170.

Kouza, M., Hansmann, UHE. 2011. Velocity scaling for optimizing replica exchange molecular dynamics. *J. Chem. Phys*., 134: (044124) 1-6.

Limongelli, V., Marinelli, L., Coscanati, S., La Motta, C., Sartini, S., Mugnaini, L., Da Settimo, F., Novellino, E., Parrinello, M. 2012. Sampling Protein Motion and Solvent Effect During Ligand Binding. *Proc. Natl. Acad. Sci*., 109: 1467-1472.

Lin, HC., Tsai, WC. 2003. Piezoelectric crystal immunosensor for the detection of staphylococcal enterotoxin B. *Biosens. Bioelectron*, 18: 1479–1483.

Maisuradze, GG., Leitner, DM. 2007. Free Energy Landscape of a Biomolecule in Dihedral Principal Component Space: Sampling Convergence and Correspondence Between Structures and Minima. *PROTEİNS*, 67: 569-578.

Maisuradze, GG., Liwo, A., Schrega, HA. 2009. How Adequate are one and two dimensional free energy landscapes for protein folding dynamics. *Phys. Rev. Lett.*, 102: (238102) 1-4.

Marrack, P., Kappler, J. 1990. The staphylococcal enterotoxins and their relatives. *Science*, 248: 705–711.

Mobley, DL., Bayly, CL.. Cooper, MD., Shirts, MR., Dill, KA. 2009. Small Molecule Hydration Free Energies in Explicit Solvent: An Extensive Test of Fixed-Charge Atomistic Simulations. *J. Chem. Theory Comput*., 5: 350-358.

Mobley, DL., Klimovich, PV. 2012. Perspective: Alchemical Free Energy Calculations for Drug Discovery. *J. Chem. Phys*., 137: 230901.

Naimushin, AN., Soelberg, SD., Nguyen, DK., Dunlap, L., Bartholomew, D., Elkind, J., Melendez, J., Furlong, C.E. 2002. Detection of Staphyloccoccus aureus enterotoxin B at femtomolar levels with a miniature integrated two channel surface plasmon resonance (SPR) sensor. *Biosens. Bioelectron*, 17: 573–584.

Nemety, G., Scheraga, HA. 1962. The Structure of Water and Hydrophobic Bonding in Proteins III. The Thermodynamic Properties of Hydrophobic Bonds in Proteins. *J. Phys. Chem*., 66(10): 1773-1789.

Pace, CN., Shirley, BA., Mcnutt, M., Gajiwala, K. 1996. Forces contributing to the conformational stability of proteins. *FASEB J*., 10: 75-83.

Park, CE., Akhtar, M., Rayman, MK. 1994. Evaluation of a commercial enzyme immunoassay kit (RIDASCREEN) for detection of staphylococcal enterotoxins A, B, C, D, and E in foods. *Appl. Environ. Microb*., 60: 677–681.

Patriksson, A., van der Spoel, D.A. 2008. Temperature predictor for parallel tempering simulations. *Phys. Chem.*, 10: 2073-2077.

Ren, P., Ponder, J.W. 2002. Consistent treatment of inter- and intramolecular polarization in molecular mechanics calculations. *J. Comp. Chem*., 23: 1497-1506.

Slavik, R., Homola, J., Brynda, E. 2002. A miniature fiber optic surface plasmon resonance sensor for fast detection of Staphyloccoccal enterotoxin B. *Biosens. Bioelectron*., 17: 591–595.

Sugita, Y., Okamoto, Y. 1999. Replica-exchange molecular dynamics method for protein folding. *Chem. Phys. Lett.*, 314: 141-151.

Swendsen, R., Wang, J. 1986. Replica Monte Carlo of spin-glasses. *Phys. Rev. Lett*., 57: 2607-2609.

Swift, RV., Amaro, RE. 2013. Back to the Future: Can Physical Models of Passive Membrane Permeability Help Reduce Drug Candidate Attrition and Move Us Beyond QSPR? *Chem. Biol. Grug Des.*, 81: 61-71.

Van der Spoel, D., Lindahl, E., Hess, B., Groenhof, G., Mark, A.E., Brendsen HJ. 2005. Gromacs: Fast, Flexible, and free. *J. Comp. Chem.*, 26: 1701-1718.

Warshel, A. 1981. Calculations of Enzymic Reactions: Calculations of pKa, Proton Transfer Reactions and General Acid Catalysis Reactions in Enzymes. *Biochemistry*, 20: 3167-3177.